EKSPLOATACJA I NIEZAWODNOŚĆ MAINTENANCE AND RELIABILITY

Eksploatacja i Niezawodnosc – Maintenance and Reliability

Volume 22 (2020), Issue 4

journal homepage: http://www.ein.org.pl

Article citation info:
Gao J-X, An Z-W, Ma Q, Bai X-Z. Residual strength assessment of wind turbine rotor blade composites under combined effects of natural aging and fatigue loads. Eksploatacja i Niezawodnosc – Maintenance and Reliability 2020; 22 (4): 601–609, http://dx.doi.org/10.17531/ein.2020.4.3.

Residual strength assessment of wind turbine rotor blade composites under combined effects of natural aging and fatigue loads

Indexed by: Web of Science Group

Jian-Xiong Gao [a*], Zong-Wen An [b*], Qiang Ma [b], Xue-Zong Bai [b]

[a]School of Mechanical Engineering, Post-Doctoral Research Station of Electrical Engineering, Xinjiang University, Urumqi, 830046, P. R. China
[b]School of Mechanical and Electronical Engineering, Lanzhou University of Technology, Lanzhou, 730050, P. R. China

Highlights

- The relationship among residual strength, aging time and the CEF is quantified.
- Temperature has an important influence on the residual strength of GFRP.
- A model is proposed to account for combined effects of natural aging and fatigue loads.
- Natural aging has both positive and negative effects on the residual strength of GFRP.

Abstract

In this paper, the combined effects of natural aging and fatigue loads are considered to assess the residual strength of wind turbine rotor blade composites under actual service environments. Firstly, a comprehensive environmental factor (CEF) methodology is adopted to quantify the combined effects of environmental factors on residual strength. Meanwhile, the artificial accelerated aging test data are used to determine the weight coefficients of the CEF. Subsequently, a two-variable function is presented to characterize the relationship among residual strength, aging time and the CEF. The natural aging test data are utilized to estimate the unknown parameters of the two-variable function. Finally, the combined effects of natural aging and fatigue loads are considered, and a residual strength model is proposed to analyze the strength degradation behaviors of the wind turbine rotor blade composites. The results indicate that fatigue loads have negative effect on the residual strength, while natural aging has both positive and negative effects on the residual strength.

Keywords

wind turbine rotor blade, natural aging, fatigue loads, residual strength, composite material.

Acronyms and Abbreviations

GFRP	Glass fiber reinforced polymer.
CEF	Comprehensive environmental factor.

Notations

k	Value of CEF.
T	Temperature.
H	Heat-humidity.
U	Ultraviolet radiation.
w_i	Weight coefficient.
S_0	Initial strength.
t_0	Initial time.
S_i	Residual strength at time t_i.
$S_{r1}(t,k)$	Residual strength under natural aging.
a_i	Parameter of $S_{r1}(t,k)$.
$S_{r2}(n,\sigma_{max})$	Residual strength under fatigue loads.
α	Parameter of $S_{r2}(n,\sigma_{max})$.
β	Parameter of $S_{r2}(n,\sigma_{max})$.
m	Parameter of σ-N curve.
C	Parameter of σ-N curve.
λ	Parameter related to load type.
n	Load cycles.
σ_{max}	Maximum stress.
N	Fatigue life.
$\Delta S_1(n,k)$	Strength degradation caused by natural aging.
$\Delta S_2(n,\sigma_{max})$	Strength degradation caused by fatigue loads.
$S_r(n,k,\sigma_{max})$	Residual strength affected by both natural aging and fatigue loads.

1. Introduction

Wind energy is one of the most representative renewable energies, which plays an important role in reducing the dependency of human beings on fossil energy. In recent decades, the development of wind power generation technology enables wind energy has becoming a pillar of the energy systems in many countries [12, 27, 37].

(*) Corresponding author.
E-mail addresses: J-X Gao - jianxionggao@xju.edu.cn, Z-W An - anzw@lut.edu.cn, Q Ma - maqiang_lut@qq.com, X-Z Bai, 15101256903@163.com

Wind turbine rotor blades, typically made by glass fiber reinforced polymer (GFRP), are the key components of wind turbines [1, 18]. Because GFRP has adequate strength and stiffness, superior durability, good damage tolerance property, it has been widely used in the fields of aerospace, mechanical, construction, and marine engineering [8, 25, 36]. Wind turbine rotor blades are long-lifetime (at least 20 years) and high-reliability components [19]. Harsh environmental conditions make the natural aging of wind turbine rotor blades inevitable. The natural aging process of GFRP is caused by oxygen, temperature, moisture, and sunlight, etc. These factors have great effects on the mechanical properties of GFRP, such as strength and stiffness degradations. Such degradations directly lead to the premature failures of wind turbine rotor blades. Moreover, the stochastic wind speed endows wind turbine rotor blades highly uncertain fatigue loads during the long periods of service [17, 28, 30]. Accordingly, fatigue damage of GFRP gradually increases over time, and fatigue failure will occur when accumulated fatigue damage reaches a certain extent. In general, fatigue fracture of wind turbine rotor blades will cause serious economic loss and catastrophic accidents.

The durability of wind turbine rotor blade composites is a serious issue from both the economic and safety point of views [11, 13, 21]. Over the past few decades, researchers have paid much attention to the natural aging and fatigue failure of composites. For instance, Vu et al. [32] carried out an artificial accelerated aging test to investigate the thermal-oxidation aging behaviors of composites from a microscopic scale, and the test results indicated that the thermal-oxidation aging process of composites strongly depends on aging time, distances between fibers and partial oxygen pressure. Mouzakis et al. [23] presented an approach for damage assessment of composites under accelerated aging condition, and the validity of the presented approach was verified through stochastic model-based analysis. Kollia et al. [9] conducted an experiment to analyze the degradation mechanisms of composites under hydrothermal aging condition, and the experimental results indicated that the dominant degradation mechanisms include matrix cracking and fiber/matrix interface debonding. Wang et al. [33] focused on the durability of GFRP under accelerated aging condition, and found that the strength degradation of GFRP shows two distinct stages. Li et al. [14] explored the mechanical properties of GFRP under natural aging condition, and concluded that the bending strength of GFRP is the most sensitive indicator for natural aging process. Mu et al. [24] proposed a new pair of fatigue damage models based on an assumption that fatigue damage characterized by residual strength and residual stiffness are equal. Cheng and Hwu [4] proposed a residual strength model for fatigue life prediction of composites, and a fatigue reliability analysis approach was developed based on two-parameter Weibull distribution. Lambert et al. [10] investigated the failure mechanisms of GFRP based on the computed tomography, and the results showed that there is a significant correlation between the largest void and fatigue life. D'Amore et al. [5] analyzed the fatigue life data and residual strength data of composites, and concluded that both fatigue life and residual strength are related to its static strength. Paramonov et al. [25] introduced residual Daniels function and Daniels sequence to estimate the residual strength of composites, and then proved the existence of fatigue limit. Yao et al. [35] presented a residual strength model to quantify fatigue damage accumulation of composites, and the fatigue test data of fiber reinforced polymer were used to verify its validity.

The existing studies mentioned above have made progresses on the durability of composites. But it should be noted that these studies only focused on either natural aging or fatigue failure of composites. As a matter of fact, wind turbine rotor blade composites (i.e. GFRP) is subjected to both natural aging and fatigue loads during its long periods of service. To this end, the combined effects of natural aging and fatigue loads should be considered. In this paper, the concept of comprehensive environmental factor (CEF) is introduced to quantify the combined effects of temperature, ultraviolet radiation, and heat-humidity on residual strength of GFRP; Subsequently, a two-variable function is presented to characterize the relationship among residual strength, aging time, and the CEF; Finally, a residual strength model is proposed to account for the combined effects of natural aging and fatigue loads, and the strength degradation behaviors of GFRP are analyzed.

The rest of this paper is organized as follows. In Section 2, the CEF is introduced to quantify the combined effects of different environmental factors, and the strength degradation rule of wind turbine rotor blade composites (i.e. GFRP) under natural aging is analyzed. In Section 3, the evolution process of fatigue damage is elaborated, and the Yao's model is adopted to characterize the strength degradation behavior of GFRP under fatigue loads. In Section 4, the combined effects of natural aging and fatigue loads are considered, and the strength degradation of GFRP under actual service environment is investigated. Some corresponding conclusions are presented in Section 5.

2. Residual strength affected by natural aging

when GFRP is exposed to a specific natural environment for a long period of time, its mechanical properties (such as strength and stiffness) will change over time. Under such circumstances, the durability and safety of wind turbine rotor blade will be reduced due to the effects of various environmental factors. In this section, the strength degradation behaviors of GFRP under different environmental conditions are investigated. It had been confirmed that the bending strength is the most sensitive indicator for natural aging process of GFRP [14]. In this paper, the natural aging test data and artificial accelerated aging test data are used to investigate the strength degradation rule of wind turbine rotor blade composites. The test conditions and test results are as follows [14].

2.1. Natural aging test

Natural aging test is carried out to explore the combined effects of environmental factors on composites. Generally, the specimens are exposed to the natural environment for a period of time, then the mechanical properties of these specimens will be tested. The natural aging test of GFRP is carried out according to Chinese Standard GB/T 2573-1989. The test position covers six different regions of China, namely Xishuangbanna, Wanning, Xiamen, Lasa, Mohe and Jinan, respectively. As a matter of fact, the environmental conditions of these six regions are representative in China. Firstly, the GFRP specimens are exposed to the natural environment for a period of time, and the exposure angle is 45°of the South; Subsequently, the bending strengths of these specimens are measured on the RGT-10A testing machine, and the loading rate is 2mm/min. The test results are shown in Table 1.

Table 1. Test results of natural aging

Time (Month)	Residual strength (MPa)					
	XSBN	WN	XM	LS	MH	JN
0	609	609	609	609	609	609
0.5	690	615	691	643	643	636
1	603	616	676	616	681	645
2	552	641	700	606	671	652
3	668	619	584	621	626	687
6	629	624	561	592	645	573
9	645	606	616	609	645	628
12	589	620	597	627	670	560
18	553	441	618	545	599	547
24	531	475	565	541	608	599
36	475	419	553	500	540	531

Note that the abbreviations of 'XSBN', 'WN', 'XM', 'LS', 'MH', and 'JN' represent the regions of 'Xishuangbanna', 'Wanning', 'Xiamen', 'Lasa', 'Mohe', and 'Jinan', respectively.

According to Table 1, the scatter plot of natural aging test data of wind turbine rotor blade composites (i.e. GFRP) can be obtained, as shown in Fig. 1.

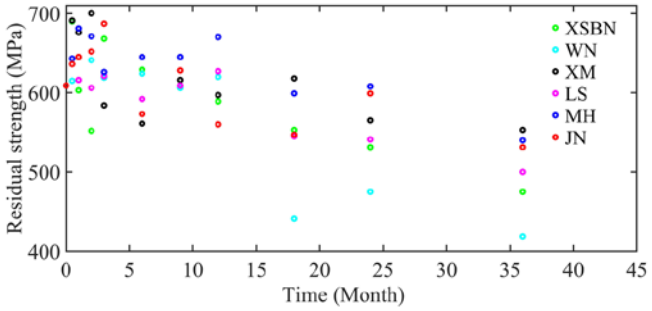

Fig. 1. Scatter plot of natural aging test data of GFRP

Fig. 1 shows that the initial bending strength of GFRP is 609MPa, then it gradually changes over time. The bending strength of GFRP increases at the early stage, then it gradually decreases at the later stages. For a specific time, the bending strengths of GFRP specimens in six test positions scatter on a large range. According to the uncertainty results from material variability and usage load variation of engineering components [2, 16, 22, 38, 39], the internal defect that derived from manufacturing process is one of the main reasons, such as bubbles, inclusions, bent fibers, resin-deficient and resin-rich areas. The other reason is that the environmental conditions in these six test positions are very different.

2.2. Artificial accelerated aging test

Artificial accelerated aging test refers to the aging processes accelerated by simulation of outdoor environments in the laboratory. Many experiments had proved that temperature, ultraviolet radiation and heat-humidity are three most critical environmental factors affecting the aging process of composites [14]. However, it should be noted that these environmental factors have different effects on mechanical properties of composites. To quantify the effect of each environmental factor on the bending strength of GFRP, three kinds of artificial accelerated aging tests are carried out, namely temperature accelerated aging test, ultraviolet radiation accelerated aging test, and heat-humidity accelerated aging test, respectively.

The temperature accelerated aging test is carried out according to Chinese Standard GB/T 7141-1992, the test temperature is 80. The ultraviolet radiation accelerated aging test is carried out according to Chinese Standard GB/T 164222.2-1999, the radiation intensity is 0.50W/m^2 and the wavelength is 340nm. The heat-humidity accelerated aging test is carried out according to Chinese Standard GB/T 2574-1989, the test temperature is 60 and the relative humidity is 95%. When the accelerated aging test is carried out for a period of time, the bending strengths of GFRP specimens are measured on the

Table 2. Test results of artificial accelerated aging

Temperature		Ultraviolet radiation		Heat-humidity	
Time (h)	Bending strength (MPa)	Time (h)	Bending strength (MPa)	Time (h)	Bending strength (MPa)
0	609	0	609	0	609
24	627	50	596	24	617
72	633	80	659	48	664
144	691	150	700	144	681
240	675	300	682	336	665
360	709	500	658	504	633
600	670	720	687	672	661
840	665	960	597	840	657
1080	623	1200	628	1176	612
1440	633	1500	593	1512	620
1800	649	1800	601	2016	578

Table 3. Estimation of weight coefficients of the CEF

Temperature			Ultraviolet radiation			Heat-humidity		
t_i (h)	S_i (MPa)	$(S_i\text{-}S_0)/(t_i\text{-}t_0)$	t_i (h)	S_i (MPa)	$(S_i\text{-}S_0)/(t_i\text{-}t_0)$	t_i (h)	S_i (MPa)	$(S_i\text{-}S_0)/(t_i\text{-}t_0)$
24	627	0.7500	50	596	-0.2600	24	617	0.3333
72	633	0.3333	80	659	0.6250	48	664	1.1458
144	691	0.5694	150	700	0.6067	144	681	0.5000
240	675	0.2750	300	682	0.2433	336	665	0.1667
360	709	0.2778	500	658	0.0980	504	633	0.0476
600	670	0.1017	720	687	0.1083	672	661	0.0774
840	665	0.0667	960	597	-0.0125	840	657	0.0571
1080	623	0.0130	1200	628	0.0158	1176	612	0.0026
1440	633	0.0167	1500	593	-0.0107	1512	620	0.0073
1800	649	0.0222	1800	601	-0.0044	2016	578	-0.0154
Mean value		0.2426	Mean value		0.1410	Mean value		0.2322

RGT-10A testing machine, and the loading rate is 2mm/min. The test results are shown in Table 2.

2.3. Comprehensive environmental factor

Table 2 shows that the effects of temperature, ultraviolet radiation and heat-humidity on the bending strength of wind turbine rotor blade composites (i.e. GFRP) are different. Here, the concept of CEF is adopted to quantify the combined effects of these three environmental factors, as shown in equation (1):

$$k = f(T,H,U) = w_1 T + w_2 H + w_3 U \tag{1}$$

where k is the CEF; T represents temperature; H represents heat-humidity; U represents ultraviolet radiation; $f(T,H,U)$ is a function of T, H and U; w_i $(i=1,2,3)$ is the weight coefficient and its value illustrates the importance of each environmental factor.

The effects of three environmental factors on the strength degradation rate of GFRP are different. Therefore, the weight coefficients of the CEF can be estimated based on the strength degradation rate of GFRP under each environmental factor, as shown in Table 3.

In Table 3, S_0 represents the initial bending strength of GFRP, and its value equals 609MPa; t_0 represents the initial time and its value equals 0; S_i represents the residual strength of GFRP at time t_i; $(S_i\text{-}S_0)/(t_i\text{-}t_0)$ represents the strength degradation rate of GFRP within time interval $[t_0,t_i]$. Table 3 indicates that the mean values of strength degradation rate of GFRP under these three environmental factors are 0.2426, 0.1410 and 0.2322, respectively. Therefore, the weight coefficients of the CEF can be determined, as shown in equation (2):

$$\begin{cases} w_1 = 0.2426/(0.2426+0.1410+0.2322) = 0.3939 \\ w_2 = 0.2322/(0.2426+0.1410+0.2322) = 0.3772 \\ w_3 = 0.1410/(0.2426+0.1410+0.2322) = 0.2289 \end{cases} \tag{2}$$

According to equation (2), the CEF can be written as follows:

$$k = 0.3939T + 0.3772H + 0.2289U \tag{3}$$

From equation (3) we have $w_1 > w_2 > w_3$, which indicates that the temperature has the strongest effect on residual strength of GFRP, then is the heat-humidity and ultraviolet radiation. According to equation (3), the CEFs of six test positions can be figured out, as shown in Table 4.

Table 4 indicates that the CEFs of the six test positions differ greatly from each other. The minimum and maximum values of the CEF are 1024.2 and 1766.1, respectively. In essence, the dispersion between the CEFs reflects the large differences between environmental conditions in these six test positions.

2.4. Strength degradation caused by natural aging

Suppose the residual strength of GFRP under natural aging conditions is denoted as S_{r1}. Generally, S_{r1} is considered as a two-variable function of k and t, denoted as $S_{r1}(t,k)$. The natural aging process is affected by many environmental factors, which makes the natural aging mechanisms of GFRP very complicated [20, 29, 33]. From the perspective of micro-mechanism, there are still many difficulties in establishing analytical expression of $S_{r1}(t,k)$ with clear physical meaning. In this paper, a mathematical model is proposed to quantify the relationship among residual strength, aging time and the CEF, as shown in equation (4):

$$S_{r1}(t,k) = S_0 + (a_0 + a_1 \cdot t + a_2 \cdot k) \cdot [\ln(1 + k \cdot t)]^{1/2} \tag{4}$$

where a_0, a_1 and a_2 are three undetermined parameters, which can be estimated through the regression analysis approach.

There are six groups of test data in Table 1, and each group of test data contains eleven samples. Combined with the CEFs of six test positions in Table 4, 66 sample data (S_{r1i}, t_i, k_i) ($i=1,2,3,\cdots,66$) can be used to estimate the undetermined parameters in equation (4), as shown in Table 5.

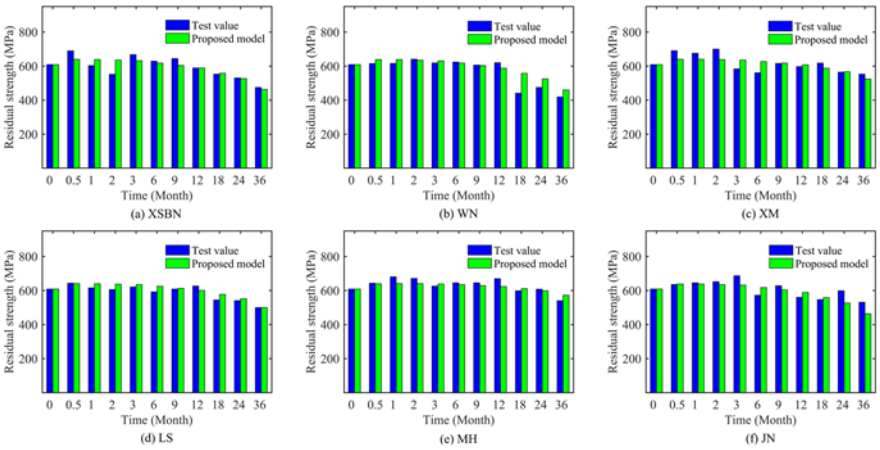

Fig. 2. Comparison between calculation results and test values

Table 4. The CEFs of six test positions

Test positions	Average annual temperature	Average annual relative humidity (%)	Annual total radiation (MJ·m^{-2})	k
XSBN	21.4	82	5490	1296.0
WN	24.5	86	4826	1146.8
XM	21.0	83	5237	1238.3
LS	7.4	34	7647	1766.1
MH	-3.5	58	4385	1024.2
JN	14.5	60	4868	1142.6

Table 5. Sample data

i	S_{r1i} (MPa)	t_i (Month)	k_i
1	609	0	1296.0
2	690	0.5	1296.0
3	603	1	1296.0
...	...	...	...
66	531	36	1142.6

According to Table 5, parameters a_0, a_1 and a_2 can be determined through the regression analysis approach. The parameter estimation results are as follows:

$$\begin{cases} a_0 = 25.36 \\ a_1 = -1.30 \\ a_2 = -0.01 \end{cases} \tag{5}$$

To verify the calculation accuracy of the proposed model, the calculation results are compared with the natural aging test data in Table 1. The comparison results are shown in Fig. 2 and Table 6.

Fig. 2 shows that the calculation results of the proposed model agree well with the natural aging test data in six test positions. According to Table 6, the average relative error of the proposed model is 4.84%<5%, while the average relative error of the existing model in Ref. [14] is 5.38%>5%. Therefore, the proposed model is more accuracy than the existing model in Ref. [14].

3. Residual strength affected by fatigue loads

Due to the cumulative damage caused by fatigue loads, the mechanical properties of wind turbine rotor blades gradually decrease during the long periods of service. In general, fatigue damage accumulation of GFRP is a complex process, which involves many different damage mechanisms, such as matrix cracking, fiber/matrix interface debonding and fiber fracture [34]. Many experiments have confirmed that the development of fatigue damage in composites con-

Table 6. Calculation accuracy analysis of the proposed model

Test positions	Aging time (Month)	Test value (MPa)	Proposed model (MPa)	Relative error (%)	Test positions	Aging time (Month)	Test value (MPa)	Proposed model (MPa)	Relative error (%)
XSBN	0	609	609	0	LS	0	609	609	0
	0.5	690	639	7.39		0.5	643	627	2.49
	1	603	639	5.97		1	616	626	1.62
	2	552	636	15.22		2	606	624	2.97
	3	668	633	5.24		3	621	620	0.16
	6	629	623	0.95		6	592	609	2.87
	9	645	611	5.27		9	609	597	1.97
	12	589	599	1.70		12	627	584	6.86
	18	553	574	3.80		18	545	558	2.39
	24	531	549	3.39		24	541	532	1.66
	36	475	496	4.42		36	500	479	4.20
WN	0	609	609	0	MH	0	609	609	0
	0.5	615	642	4.39		0.5	643	645	0.31
	1	616	642	4.22		1	681	645	5.29
	2	641	640	0.16		2	671	644	4.02
	3	619	638	3.07		3	626	641	2.40
	6	624	627	0.48		6	645	631	2.17
	9	606	616	1.65		9	645	619	4.03
	12	620	604	2.58		12	670	608	9.25
	18	441	579	31.29		18	599	583	2.67
	24	475	554	16.63		24	608	558	8.22
	36	419	502	19.81		36	540	506	6.30
XM	0	609	609	0	JN	0	609	609	0
	0.5	691	640	7.38		0.5	636	642	0.94
	1	676	640	5.33		1	645	643	0.31
	2	700	638	8.86		2	652	641	1.69
	3	584	635	8.73		3	687	638	7.13
	6	561	624	11.23		6	573	627	9.42
	9	616	613	0.49		9	628	616	1.91
	12	597	601	0.67		12	560	604	7.86
	18	618	576	6.80		18	547	579	5.85
	24	565	551	2.48		24	599	554	7.51
	36	553	498	9.95		36	531	502	5.46

sists of (a) transverse matrix cracking followed by longitudinal matrix cracking (Stages 1 and 2), (b) local delamination between adjacent layers (Stage 3), and (c) fiber breakage of the 0° plies (Stages 4 and 5), as shown in Fig. 3 [31].

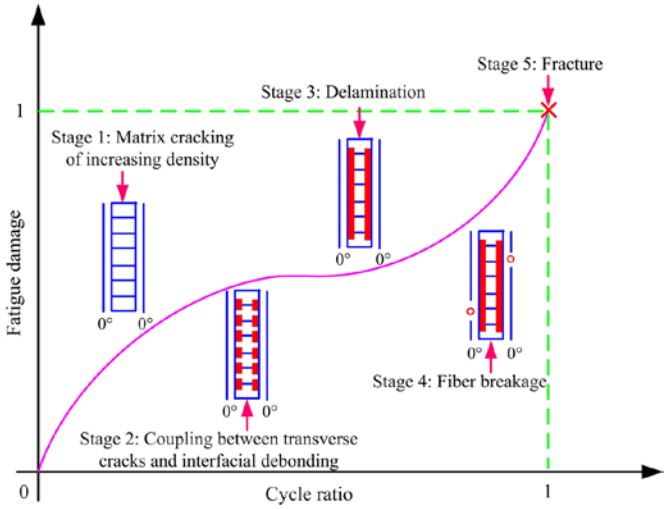

Fig. 3. Development of fatigue damage in composites

Fig. 3 indicates that fatigue damage accumulation of composites shows a fast-slow-fast trend during the fatigue process. To quantify such characteristics of fatigue damage accumulation, the Yao's model is adopted to characterize the strength degradation behavior of GFRP under fatigue loads, as shown in equation (6) [35]:

$$S_{r2}(n,\sigma_{max}) = S_0 - (S_0 - \sigma_{max}) \cdot \left[\frac{\sin(\beta \cdot \frac{n}{N}) \cdot \cos(\beta - \alpha)}{\sin(\beta) \cdot \cos(\beta \cdot \frac{n}{N} - \alpha)} \right] \quad (6)$$

where $S_{r2}(n,\sigma_{max})$ represents the residual strength under fatigue loads, which is a two-variable function of loading times n and maximum stress σ_{max}; N is the fatigue life under stress σ_{max}; α and β are two undetermined parameters of the model. In practical applications, if the test data on residual strength of composites are not available, it is recommended that $\beta = \frac{2\pi}{3}$ and $\alpha = \frac{\beta}{2}$ [35].

To analyze the strength degradation rule of wind turbine rotor blade composites (i.e. GFRP) under fatigue loads, the fatigue life N under stress σ_{max} should be determined. Generally, fatigue life N under stress σ_{max} can be figured out based on the σ-N curve. The σ-N curve is usually expressed as the power law formula, as shown in equation (7) [6, 15]:

$$\sigma_{max}^{m} \cdot N = C \quad (7)$$

where m and C are two undetermined parameters.

According to equation (7), fatigue life N can be formulated as follows:

$$N = \frac{C}{\sigma_{max}^{m}} \quad (8)$$

When parameters m and C are known, fatigue life N of GFRP under stress σ_{max} can be easily figured out. In engineering applications, when experimental data on fatigue life are not available, parameters m and C can be estimated through the following approach [3].

When the maximum stress σ_{max} equals $0.9S_0$, the corresponding fatigue life N equals 10^3 cycles; When the maximum stress σ_{max} equals λS_0, the corresponding fatigue life N equals 10^6 cycles. Parameter λ is related to the loading type. λ equals 0.29 under the torsion loading, λ equals 0.35 under the tension or compression loading, λ equals 0.5 under the bending loading. According to this principle and equation (7), we can get:

$$\begin{cases} (0.9S_0)^m \times 10^3 = C \\ (\lambda S_0)^m \times 10^6 = C \end{cases} \quad (9)$$

According to equation (9), parameters m and C can be formulated as follows:

$$\begin{cases} m = \dfrac{3}{\lg(\frac{0.9}{\lambda})} \\ C = (0.9S_0)^m \times 10^6 \end{cases} \quad (10)$$

As mentioned above, the initial bending strength of wind turbine rotor blade composites (i.e. GFRP) is 609MPa, namely $S_0 = 609\text{MPa}$. Moreover, the σ-N curve under the bending loading is needed, so $\lambda = 0.5$. According to equation (10), parameters m and C can be figured out:

$$\begin{cases} m = \dfrac{3}{\lg(\frac{0.9}{0.5})} = 11.7521 \\ C = (0.9 \times 609)^{11.7521} \times 10^6 = 1.5394 \times 10^{38} \end{cases} \quad (11)$$

Equation (11) indicates that parameters m and C have been completely determined. Therefore, fatigue life of GFRP under any stress level can be figured out based on equation (8). For example, if the maximum stress σ_{max} equals 400MPa, the corresponding fatigue life N equals 4.0521×10^7 cycles. According to equation (6), the corresponding residual strength curve of GFRP can be obtained, as shown in Fig. 4.

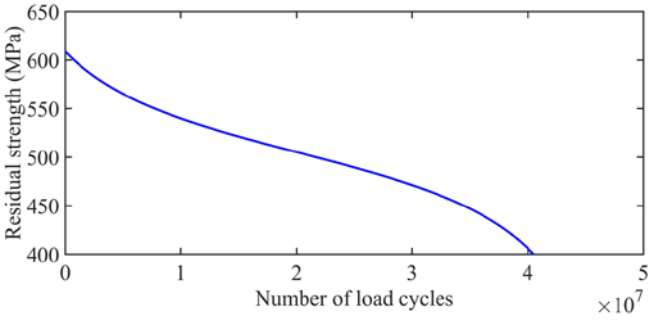

Fig. 4. Residual strength curve of GFRP when σ_{max}=400MPa

Fig. 4 indicates that the strength degradation rule of wind turbine rotor blade composites (i.e. GFRP) is consistent with the development of fatigue damage shown in Fig. 3. This phenomenon indicates that the Yao's model can accurately characterize the strength degradation rule of GFRP under fatigue loads.

4. Residual strength affected by both natural aging and fatigue loads

In practical engineering, wind turbine rotor blades are subjected to both natural aging and fatigue loads during the long periods of service. Therefore, it is necessary to account for the combined effects of natural aging and fatigue loads during the analysis process. In this section, a residual strength model is developed to quantify the combined effects of natural aging and fatigue loads.

In general, time t is a function of the number of load cycles n, that is $t = f(n)$. Therefore, equation (4) can be written as the following form:

$$S_{r1}(n,k) = S_0 + \left[a_0 + a_1 \cdot f(n) + a_2 \cdot k\right] \times \left\{\ln\left[1 + k \cdot f(n)\right]\right\}^{1/2} \quad (12)$$

According to equation (12), the strength degradation caused by natural aging can be formulated as follows:

$$\begin{aligned} \Delta S_1(n,k) &= S_0 - S_{r1}(n,k) \\ &= -\left[a_0 + a_1 \cdot f(n) + a_2 \cdot k\right] \times \left\{\ln\left[1 + k \cdot f(n)\right]\right\}^{1/2} \end{aligned} \quad (13)$$

where $\Delta S_1(n,k)$ represents the strength degradation caused by natural aging, which is a two-variable function of the number of load cycles n and CEF k.

According to equation (6), the strength degradation caused by fatigue loads can be formulated as follows:

$$\begin{aligned} \Delta S_2(n,\sigma_{\max}) &= S_0 - S(n,\sigma_{\max}) \\ &= (S_0 - \sigma_{\max}) \cdot \left[\frac{\sin(\beta \cdot \frac{n}{N}) \cdot \cos(\beta - \alpha)}{\sin(\beta) \cdot \cos(\beta \cdot \frac{n}{N} - \alpha)}\right] \end{aligned} \quad (14)$$

where $\Delta S_2(n,\sigma_{\max})$ represents the strength degradation caused by fatigue loads, which is a two-variable function of the number of load cycles n and maximum stress $\sigma_{\max}$.

According to equations (13) and (14), a residual strength model is established to account for the combined effects of natural aging and fatigue loads, as shown in equation (15):

$$\begin{aligned} S_r(n,k,\sigma_{\max}) &= S_0 - [\Delta S_1(n,k) + \Delta S_2(n,\sigma_{\max})] \\ &= S_0 + \left[a_0 + a_1 \cdot f(n) + a_2 \cdot k\right] \times \left\{\ln\left[1 + k \cdot f(n)\right]\right\}^{1/2} - (S_0 - \sigma_{\max}) \times \left[\frac{\sin(\beta \cdot \frac{n}{N}) \cdot \cos(\beta - \alpha)}{\sin(\beta) \cdot \cos(\beta \cdot \frac{n}{N} - \alpha)}\right] \end{aligned} \quad (15)$$

where $S_r(n,k,\sigma_{\max})$ represents the residual strength affected by both natural aging and fatigue loads, which is a three-variable function of the number of load cycles n, CEF k and maximum stress $\sigma_{\max}$.

When $\sigma_{\max}$ equals 400MPa and the loading frequency is one time per second, the residual strength curves of GFRP in six test positions can be obtained based on equation (15), as shown in Fig. 5.

Fig. 5 indicates that the residual strength under fatigue loads (i.e. the blue curves in Fig. 5) decreases monotonically with the increase of load cycles. This phenomenon indicates that fatigue loads have negative effect (i.e. damage effect) on residual strength of GFRP. The main reason is that fatigue damage accumulation of composites is an irreversible process of energy dissipation. By comparison, the residual strength under natural aging (i.e. the black curves in Fig. 5) increases at the early stage, and then decreases at the later stages. This phenomenon indicates that natural aging has both positive and negative effects (i.e. enhancement effect and damage effect) on residual strength of GFRP. The similar conclusions can also be found in Refs. [20] and [33]. The residual strength under both natural aging and fatigue loads (i.e. the red curves in Fig. 5) increases at the early stage, and then gradually decreases over time. This phenomenon characterizes the strength degradation behaviors of wind turbine rotor blade composites under the actual service environment. If the effect of natural aging is only considered, the calculation results may be risky. If the effect of fatigue loads is only considered, the calculation results may be over-conservative at the early stage, and then may be risky at the later stages.

To quantify the effects of different environmental factors on residual strength, the strength degradation curves of wind turbine rotor blade composites (i.e. GFRP) in six test positions are compared, as shown in Fig. 6.

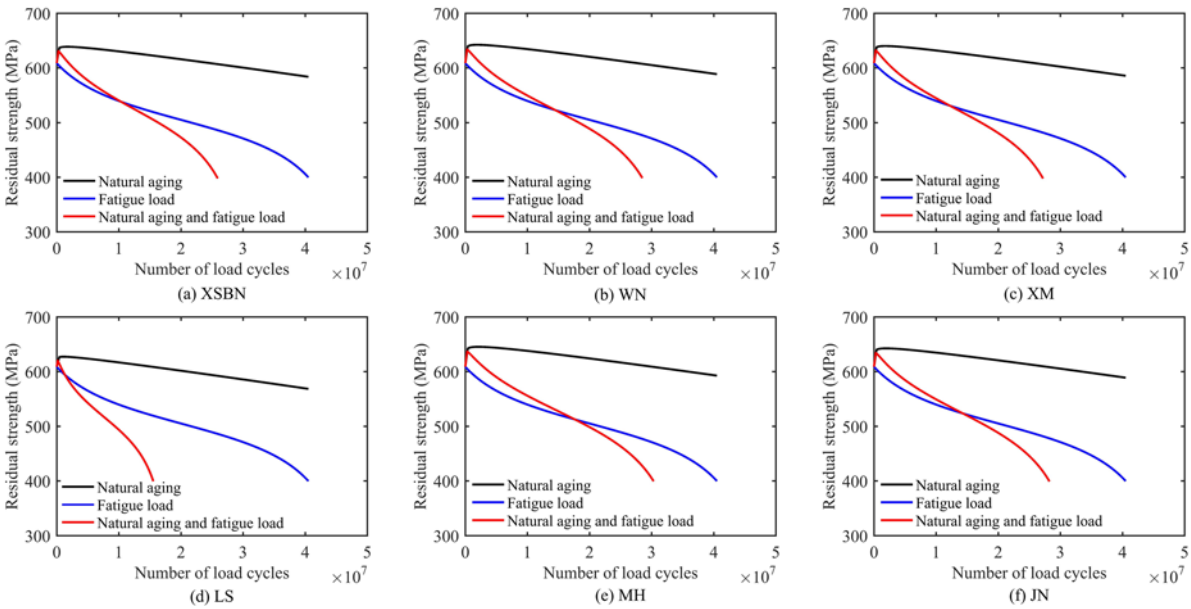

Fig. 5. Residual strength of GFRP composites in six test positions

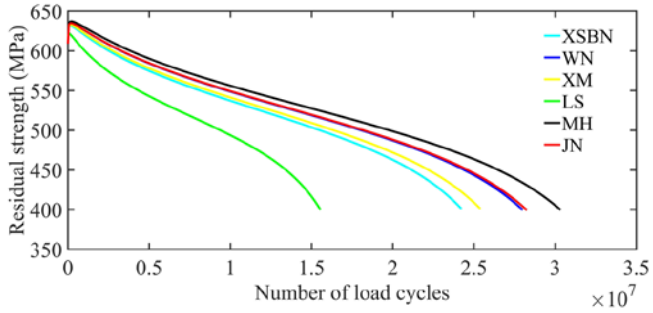

Fig. 6. Comparison of residual strength in six test positions

Fig. 6 indicates that there are significant differences between residual strength curves of wind turbine rotor blade composites (i.e. GFRP) in six test positions. By comparison, the residual strength of GFRP in MH is the highest, while the residual strength of GFRP in LS is the lowest. The main reason is that the environmental conditions in MH and LS are very different. MH is located in the northeast of China, which has a typical inland climate and the temperature is the lowest in China. LS is located in the southwest of China, which has a typical plateau climate and the solar radiation is the strongest in China. Table 4 indicates that the average annual temperatures of MH and LS are -3.5 and 7.4, respectively. The average annual relative humidities of MH and LS are 58% and 34%, respectively. The annual total radiations of MH and LS are 4385 $MJ \cdot m^{-2}$ and 7647 $MJ \cdot m^{-2}$, respectively. When GFRP is exposed to the high-temperature environment, the micro-cracks will gradually appear and in turn degrades the bending strength of GFRP. When GFRP is exposed to the heat-humidity environment, the moisture absorption may result in plastification in matrix and damage to crystalline structure [7]. The ultraviolet radiation can cause the breakage of some molecules of GFRP. The damage effect of natural aging is mainly caused by the degradations of matrix and fiber/matrix interface. The enhancement effect of natural aging is mainly caused by the stress relaxation and post-curing in GFRP.

5. Conclusions

In this paper, the CEF is introduced to quantify the combined effects of environmental factors, and the Yao's model is adopted to characterize the strength degradation of wind turbine rotor blade composites (i.e. GFRP) under fatigue loads. A residual strength model is developed to account for the combined effects of natural aging and fatigue loads, and the strength degradation rule of GFRP under actual service environment is analyzed. The results indicate that the residual strength of GFRP increases at the early stage, and then gradually decreases over time. This phenomenon shows that fatigue loads have negative effect (i.e. damage effect) on residual strength of GFRP, while natural aging has both positive and negative effects (i.e. enhancement effect and damage effect) on residual strength of GFRP. Fatigue damage accumulation of GFRP is a complex process that involves many different damage mechanisms, such as matrix cracking, fiber/matrix interface debonding and fiber fracture. Essentially, fatigue damage accumulation of GFRP is an irreversible process of energy dissipation. From the perspective of fault physics, the damage effect of natural aging is mainly caused by the degradations of matrix and fiber/matrix interface. The enhancement effect of natural aging is mainly caused by the stress relaxation and post-curing in GFRP. Compared with the existing model, the proposed model has higher calculation accuracy and the average relative error is less than 5%.

Acknowledgement

This study was supported by funds from the National Natural Science Foundation of China (Grant No: 51665029), Natural Science Foundation of Xinjiang Uygur Autonomous Region (Grant No: 2020D01C056), Tianchi Doctor Project of Department of Education of Xinjiang Uygur Autonomous Region, and Start-up Foundation of Xinjiang University for Doctor.

References

1. Beauson J, Lilholt H, Brondsted P. Recycling solid residues recovered from glass fibre-reinforced composites—A review applied to wind turbine blade materials. Journal of Reinforced Plastics and Composites 2014; 33 (16): 1542-1556, https://doi.org/10.1177/0731684414537131.
2. Byon E, Ntaimo L, Ding Y. Optimal maintenance strategies for wind turbine systems under stochastic weather conditions. IEEE Transactions on Reliability 2010; 59 (2): 393-404, https://doi.org/10.1109/TR.2010.2046804.
3. Chen C Y. Fatigue and Fracture. Wuhan: Huazhong University of Science and Technology Press, 2002.
4. Cheng H C, Hwu F S. Fatigue reliability analysis of composites based on residual strength. Advanced Composite Materials 2006; 15 (4): 385-402, https://doi.org/10.1163/156855106778835212.
5. D'Amore A, Giorgio M, Grassia L. Modeling the residual strength of carbon fiber reinforced composites subjected to cyclic loading. International Journal of Fatigue 2015; 78: 31-37, https://doi.org/10.1016/j.ijfatigue.2015.03.012.
6. Gao J X, Yuan Y P. Small sample test approach for obtaining P-S-N curves based on a unified mathematical model. Proceedings of the Institution of Mechanical Engineers, Part C: Journal of Mechanical Engineering Science 2020, https://doi.org/10.1177/0954406220925845.
7. Jiang X, Kolstein H, Bijlaard F, Qiang X. Effects of hygrothermal aging on glass-fibre reinforced polymer laminates and adhesive of FRP composite bridge: Moisture diffusion characteristics. Composites, Part A: Applied Science and Manufacturing 2014; 57 (1): 49-58, https://doi.org/10.1016/j.compositesa.2013.11.002.
8. Ji Q H, Zhu P, Lu J H, Liu Z. Carbon fiber reinforced plastic fatigue performance prediction and application based on Kriging surrogate model. IEEE Transactions on Reliability 2017; 51 (2): 129-135, https://doi.org/10.16183/j.cnki.jsjtu.2017.02.001.
9. Kollia E, Loutas T, Fiamegkou E, Vavouliotis A, Kostopoulos V. Degradation behavior of glass fiber reinforced cyanate ester composites under hydrothermal ageing. Polymer Degradation and Stability 2015; 121: 200-207, https://doi.org/10.1016/j.polymdegradstab.2015.08.015.
10. Lambert J, Chambers A R, Sinclair I, Spearing S M. 3D damage characterisation and the role of voids in the fatigue of wind turbine blade materials. Composites Science and Technology 2012; 72 (2): 337-343, https://doi.org/10.1016/j.compscitech.2011.11.023.
11. Lee H G, Park J. Static test until structural collapse after fatigue testing of a full-scale wind turbine blade. Composite Structures 2016; 136: 251-257, https://doi.org/10.1016/j.compstruct.2015.10.007.
12. Li H, Guedes Soares C. Reliability analysis of floating offshore wind turbines support structure using hierarchical Bayesian network. In M. Beer and E. Zio (Eds.), Proceedings of the 29th European Safety and Reliability Conference 2019; 2489-2495, https://doi.org /10.3850/978-981-11-2724-3 0610-cd.
13. Li H, Huang H Z, Li Y F, Zhou J, Mi J, Physics of failure-based reliability prediction of turbine blades using multi-source information fusion. Applied Soft Computing 2018; 72: 624-635, https://doi.org/10.1016/j.asoc.2018.05.015.
14. Li H, Zhang L, Sun Y, Liu Y P, Wang S L, Zhang Y Z. Prediction of service life of the glass fibre reinforced composite. Engineering Plastics

Application 2011; 39 (1): 68-73, https://doi.org/10.3969/j.issn.1001-3539.2011.01.017.
15. Li X, Huang H Z, Li F, Ren L. Remaining useful life prediction model of the space station. Eksploatacja i Niezawodnosc - Maintenance and Reliability 2019; 21 (3): 501-510, http://doi.org/10.17531/ein.2019.3.17.
16. Li X, Huang H Z, Li Y F, Li Y F. Reliability evaluation for VHF and UHF bands under different scenarios via propagation loss model. Eksploatacja i Niezawodnosc-Maintenance and Reliability 2019; 21 (3): 375-383, http://doi.org/10.17531/ein.2019.3.3.
17. Li Y F, Huang H Z, Mi J, Peng W, Han X. Reliability analysis of multi-state systems with common cause failures based on Bayesian network and fuzzy probability. Annals of Operations Research 2019; DOI: https://doi.org/10.1007/s10479-019-03247-6.
18. Mandell J, Samborsky D, Wang L, Wahl N K. New fatigue data for wind turbine blade materials. Journal of Solar Energy Engineering 2003; 125 (4): 167-179, https://doi.org/10.1115/1.1624089.
19. Ma Q, An Z W, Gao J X, Kou H X, Bai X Z. A method of determining test load for full-scale wind turbine blade fatigue tests. Journal of Mechanical Science and Technology 2018; 32 (11): 5097-5104, https://doi.org/10.1007/s12206-018-1006-y.
20. Marouani S, Curtil L, Hamelin P. Ageing of carbon/epoxy and carbon/vinylester composites used in the reinforcement and/or the repair of civil engineering structures. Composites, Part B: Engineering 2012; 43 (4): 2020-2030, https://doi.org/10.1016/j.compositesb.2012.01.001.
21. Mi J, Beer M, Li Y F, Broggi M, Cheng Y. Reliability and importance analysis of uncertain system with common cause failures based on survival signature. Reliability Engineering & System Safety 2020; 106988, https://doi.org/10.1016/j.ress.2020.106988.
22. Mi J, Li Y F, Peng W, Huang H Z. Reliability analysis of complex multi-state system with common cause failure based on evidential networks. Reliability Engineering & System Safety 2018; 174: 71-81.
23. Mouzakis D E, Dimogianopoulos D G, Zaoutsos S. Damage assessment of carbon fiber reinforced composites under accelerated aging and validation via stochastic model-based analysis. International Journal of Damage Mechanics 2014; 23 (5): 702-726, https://doi.org/10.1177/1056789513508798.
24. Mu P G, Wan X P, Zhao X Y. A new pair of cumulative fatigue damage models for composite materials. Advanced Materials Research 2010; 160: 226-230, https://doi.org/10.4028/www.scientific.net/AMR.160-162.226.
25. Paramonov Y, Cimanis V, Varickis S, Kleinhofs M. Modeling the residual strength of a fibrous composite using the residual Daniels function. Mechanics of Composite Materials 2016; 52 (4): 497-506, https://doi.org/10.1007/s11029-016-9600-5.
26. Ratnaparkhi M V, Park W J. Lognormal distribution-model for fatigue life and residual strength of composite materials. IEEE Transactions on Reliability 1986; 35 (3): 312-315, https://doi.org/10.1109/TR.1986.4335440.
27. Romanski L, Bieniek J, Komarnicki P, Debowski M, Detyna J. Operational tests of a dual-rotor mini wind turbine. Eksploatacja i Niezawodnosc - Maintenance and Reliability 2016; 18 (2): 201-209, http://doi.org/10.17531/ein.2016.2.7.
28. Shafiee M, Finkelstein M, Bérenguer C. An opportunistic condition-based maintenance policy for offshore wind turbine blades subjected to degradation and environmental shocks. Reliability Engineering and System Safety 2015; 142: 463-471, https://doi.org/10.1016/j.ress.2015.05.001.
29. Shuai L, Zhencai Z, Hao L, Gang S. A system reliability-based design optimization for the scraper chain of scraper conveyors with dependent failure modes. Eksploatacja i Niezawodnosc - Maintenance and Reliability 2019; 21 (3): 392-402, http://doi.org/10.17531/ein.2019.3.5.
30. Topic D, Sljivac D, Stojkov M. Reliability model of different wind power plant configuration using sequential Monte Carlo simulation. Eksploatacja i Niezawodnosc - Maintenance and Reliability 2016; 18 (2): 237-244, http://doi.org/10.17531/ein.2016.2.11.
31. Vassilopoulos A P. Fatigue Life Prediction of Composites and Composite Structures. Woodhead Publishing, 2010.
32. Vu D Q, Gigliotti M, Lafarie-Frenot M C. Experimental characterization of thermo-oxidation-induced shrinkage and damage in polymer–matrix composites. Composites, Part A: Applied Science and Manufacturing 2012; 43 (4): 577-586, https://doi.org/10.1016/j.compositesa.2011.12.018.
33. Wang Y, Meng J, Zhao Q, Qi S H. Accelerated ageing tests for evaluations of a durability performance of glass-fiber reinforcement polyester composites. Journal of Materials Science and Technology 2010; 26 (6): 572-576, https://doi.org/10.1016/S1005-0302(10)60087-4.
34. Wu F Q, Yao W X. A fatigue damage model of composite materials. International Journal of Fatigue 2010; 32 (1): 134-138, https://doi.org/10.1016/j.ijfatigue.2009.02.027.
35. Yao W X, Himmel N. A new cumulative fatigue damage model for fibre-reinforced plastics. Composites Science and Technology 2000; 60 (1): 59-64, https://doi.org/10.1016/S0266-3538(99)00100-1.
36. Zhang Y, Vassilopoulos A P, Keller T. Fracture of adhesively-bonded pultruded GFRP joints under constant amplitude fatigue loading. International Journal of Fatigue 2010; 32 (7): 979-987, https://doi.org/10.1016/j.ijfatigue.2009.11.004.
37. Zhou H F, Dou H Y, Qin L Z, Chen Y, Ni Y Q, Ko J M. A review of full-scale structural testing of wind turbine blades. Renewable and Sustainable Energy Reviews 2014; 33 (2): 177-187, http://doi.org/10.1016/j.rser.2014.01.087.
38. Zhu S P, Foletti S, Beretta S. Probabilistic framework for multiaxial LCF assessment under material variability. International Journal of Fatigue 2017; 103: 371-385, https://doi.org/10.1016/j.ijfatigue.2017.06.019.
39. Zhu S P, Huang H Z, Peng W W, Wang H K, Mahadevan S. Probabilistic physics of failure-based framework for fatigue life prediction of aircraft gas turbine discs under uncertainty. Reliability Engineering & System Safety 2016; 146: 1-12, https://doi.org/10.1016/j.ress.2015.10.002.